

# SUPPORTING INFORMATION

## **Photoelectrochemistry by Design: Tailoring the Nanoscale Structure of Pt/NiO Composites Leads to Enhanced Photoelectrochemical Hydrogen Evolution Performance**

András Sápi<sup>a</sup>, András Varga<sup>b,c</sup>, Gergely F. Samu<sup>b,c</sup>, Dorina Dobó<sup>a</sup>, Koppány L. Juhász<sup>a</sup>, Bettina Takács<sup>b,c</sup>, Erika Varga<sup>c</sup>, Ákos Kukovecz<sup>a,d</sup>, Zoltán Kónya<sup>a,e</sup>, and Csaba Janáky<sup>b,c,\*</sup>

<sup>a</sup>Department of Applied and Environmental Chemistry, University of Szeged, Rerrich Square 1, Szeged, H-6720, Hungary

<sup>b</sup>MTA-SZTE „Lendület” Photoelectrochemistry Research Group, Rerrich Square 1, Szeged, H-6720, Hungary

<sup>c</sup>Department of Physical Chemistry and Materials Science, University of Szeged, Rerrich Square 1, Szeged, H-6720, Hungary

<sup>d</sup>MTA-SZTE „Lendület” Porous Nanocomposites Research Group, Rerrich Square 1, Szeged, H-6720, Hungary

<sup>e</sup>MTA-SZTE Reaction Kinetics and Surface Chemistry Research Group, Rerrich Square 1., Szeged H-6720, Hungary

\*Corresponding author, e-mail: [janaky@chem.u-szeged.hu](mailto:janaky@chem.u-szeged.hu)

### The anodization process:

The anodization procedures always consisted of: (i) a steady increase in the voltage until the anodization voltage was reached, (ii) the anodization at constant voltage, and (iii) the slow decrease of the applied voltage to open circuit conditions. In all cases the ramping periods were omitted from the graphs and only the constant voltage phase were plotted. Note that in these cases the current is two magnitudes higher than in the case of Ti or W anodization.<sup>1,2</sup> This indicates the favorable dissolution of the NiO during anodization.

### Anodization in the phosphate containing electrolyte (1. method):

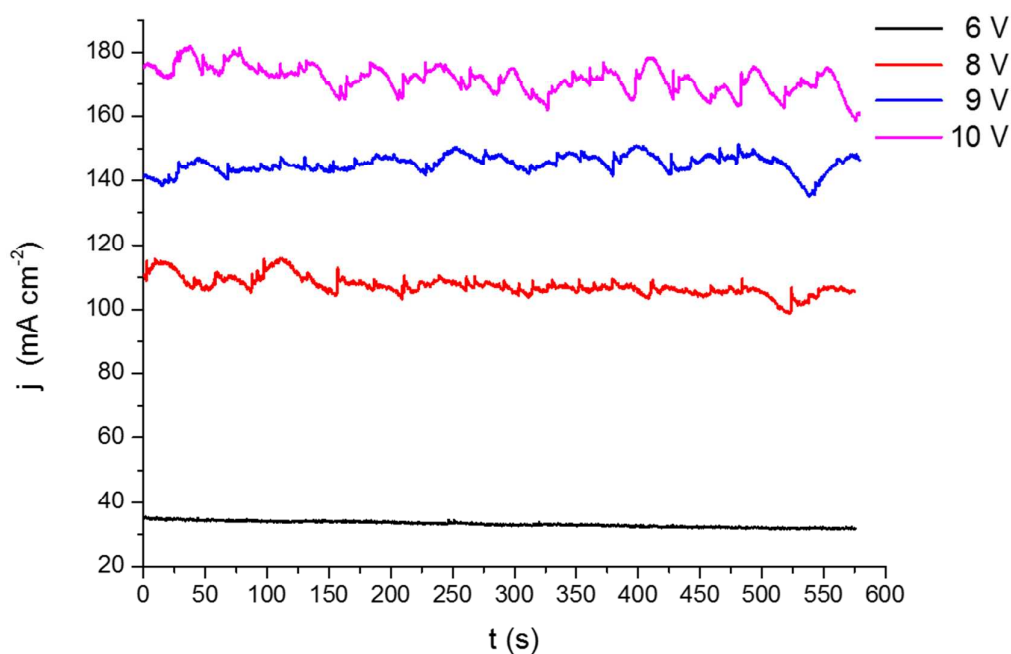


**Figure S1.** Effect of the employed voltage on the anodization curves, recorded in 0.5 M  $\text{NH}_4\text{F}$  containing 85 wt%  $\text{H}_3\text{PO}_4$  electrolyte.

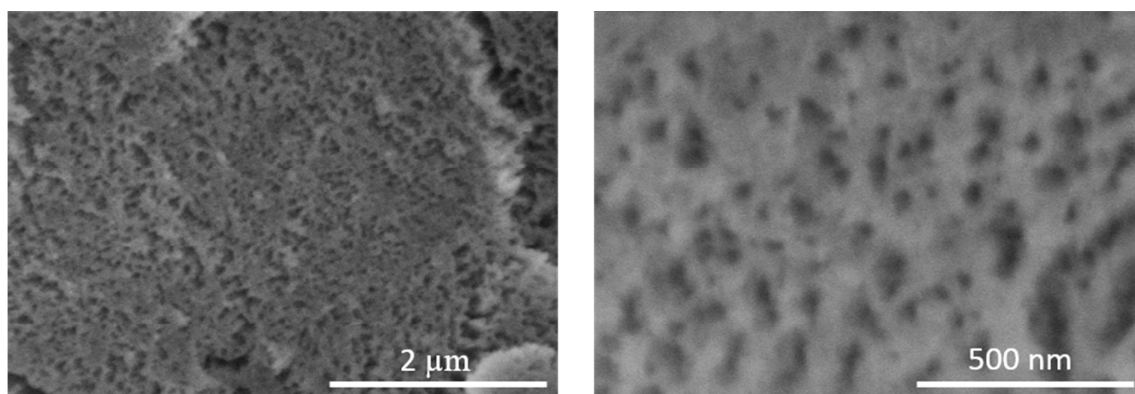


**Figure S2.** SEM images of the NiO samples obtained in 0.5 M  $\text{NH}_4\text{F}$  containing 85 wt%  $\text{H}_3\text{PO}_4$  electrolyte ( $U = 10$  V,  $t = 10$  min).

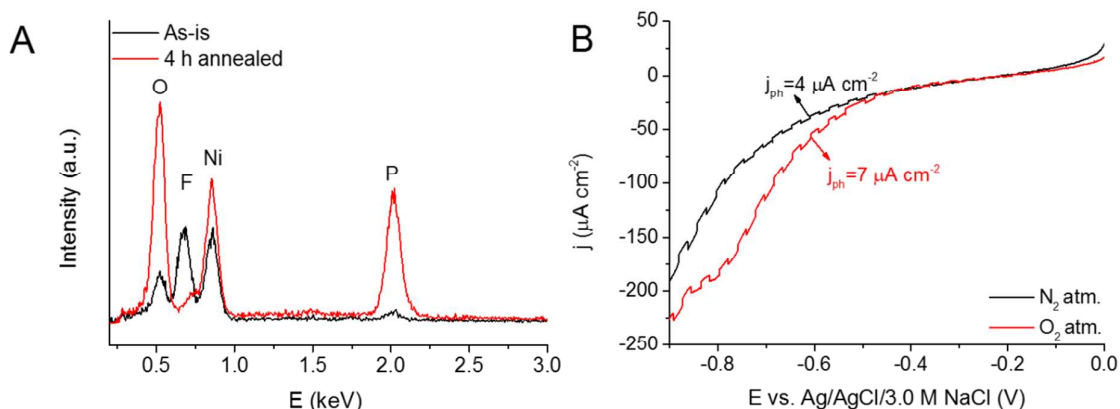


**Figure S3. A:** EDX spectra of the unannealed and annealed ( $T = 300\text{ }^{\circ}\text{C}$ , 4 h) NiO samples prepared at  $U = 10\text{ V}$ , for  $t = 10\text{ min}$ . **B:** Linear sweep photovoltammetry profiles ( $5\text{ mV s}^{-1}$ ,  $0.1\text{ Hz}$  light interruption) of the NiO sample prepared at  $U = 10\text{ V}$ , 10 min in  $0.2\text{ M Na}_2\text{SO}_4$  electrolyte in  $\text{N}_2$  and  $\text{O}_2$  saturated solutions.

It was shown previously that this method inherently produces  $\text{NiF}_2$  rich oxide layers<sup>3</sup>, because of the fluoride incorporation from the used electrolyte. However, this impurity phase can be removed by subsequent heat treatment of the film at  $300\text{ }^{\circ}\text{C}$  (as evidenced by EDX measurements Figure S3A). Intriguingly, this heat treatment step reveals a hidden drawback of this method.<sup>4</sup> As the  $\text{NiF}_2$  content of the film is removed the increase in the phosphorus and oxygen amount of the layers can be detected. This may indicate that some form of phosphate impurity (from the used electrolyte) migrates to the surface of the sample (see Figure S3A).

### Anodization in the complex electrolyte (3. method):

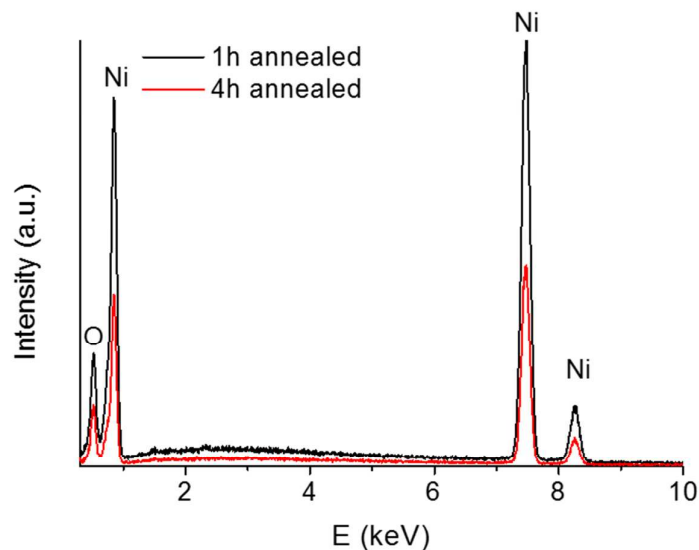


**Figure S4.** EDX spectra of the NiO samples ( $U = 30$  V, 1 h) annealed at  $T = 500^\circ\text{C}$  for different time.

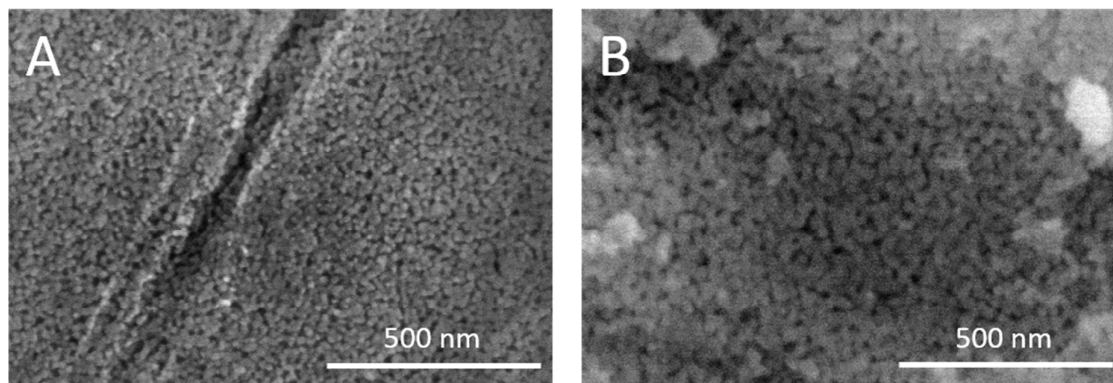


**Figure S5.** SEM image of the heat treated ( $T = 500^\circ\text{C}$ , 1h) NiO sample obtained at **A:**  $U = 40$  V, 1 h **A:**  $U = 30$  V, 1 h.

### Synthesis of Pt nanoparticles:

#### Synthesis of 2.0 nm Pt nanoparticles

For 2.0 nm Pt nanoparticles, 29 mg  $\text{PtCl}_4$  is dissolved in 2.5 ml ethylene-glycol. 2.5 ml of 0.5 M NaOH in ethylene-glycol solution were also prepared. The two solutions were mixed in a three-necked round bottom flask. After 30 minutes of sonication, the flask were evacuated and purged with atmospheric pressure argon gas in cycles to get rid of additional oxygen and water. After three purging cycles, the flask was immersed into an oil bath heated to  $160^\circ\text{C}$  under vigorous stirring of the reaction mixture as well as the oil bath. After 180

minutes of reaction, the flask was cooled down to room temperature. The pH of the suspension is neutralized with 2 M aqueous solution of HCl. After neutralization, 4 mg polyvinylpyrrolidone (PVP,  $M_w = 40,000$ ) solved in 2 ml ethanol is applied, then the suspension is precipitated with centrifuging. The nanoparticles are washed by centrifuging with hexane and redispersed in ethanol for at least 2-3 cycles, and finally stored in ethanol.

#### Synthesis of 4.8 nm Pt nanoparticles

For 4.8 nm Pt nanoparticles, 40 mg  $\text{Pt}(\text{C}_5\text{H}_7\text{O}_2)_2$  and 35 mg polyvinylpyrrolidone (PVP,  $M_w = 40,000$ ) are solved in 5 ml ethylene-glycol, and sonicated for 30 minutes to get a homogenous solution. The solution was transferred into a three-necked round bottom flask, which was evacuated and purged with atmospheric pressure argon gas to get rid of additional oxygen and water. After three purging cycles, the flask was immersed into an oil bath heated to 200 °C under vigorous stirring of the reaction mixture as well as the oil bath. After 10 minutes of reaction, the flask was cooled down to room temperature. The suspension was precipitated by adding acetone to the mixture. The nanoparticles were collected by centrifuging. After precipitation, the particles were washed by centrifuging with hexane and redispersing in ethanol for at least 2-3 cycles, and finally stored in ethanol.

#### Synthesis of 7.2 nm Pt nanoparticles

For 7.2 nm Pt nanoparticles, 41 mg  $\text{H}_2\text{PtCl}_4$  and 20 mg polyvinylpyrrolidone (PVP,  $M_w = 40,000$ ) are dissolved in 5 ml ethylene-glycol, and sonicated for 30 minutes to get a homogenous solution. The solution was transferred into a three-necked round bottom flask, which was evacuated and purged with atmospheric pressure argon gas to get rid of additional oxygen and water. After three purging cycles, the flask was immersed into an oil bath heated to 200 °C under vigorous stirring of the reaction mixture as well as the oil bath. After 120 minutes of reaction, the flask was cooled down to room temperature. The suspension was precipitated by adding acetone to the mixture. The nanoparticles were collected by

centrifuging. After precipitation, the particles were washed by centrifuging with hexane and redispersing in ethanol for at least 2-3 cycles, and finally stored in ethanol.

#### Synthesis of 8.6 nm Pt nanoparticles

For 8.6 nm Pt nanoparticles in diameter, 40 mg  $\text{H}_2\text{PtCl}_6$  and 40 mg polyvinylpyrrolidone (PVP,  $M_w = 40,000$ ) is dissolved in 2.5 ml ethylene-glycol. 2.5 ml of 0.075 M NaOH in ethylene-glycol solution were also prepared. The two solutions were mixed in a three-necked round bottom flask. After 30 minutes of sonication, the flask were evacuated and purged with atmospheric pressure argon gas in cycles to get rid of additional oxygen and water. After three purging cycles, the flask was immersed into an oil bath heated to 160 °C under vigorous stirring of the reaction mixture as well as the oil bath. After 180 minutes of reaction, the flask was cooled down to room temperature. The pH of the suspension is neutralized with 2 M aqueous solution of HCl. After the neutralization, the suspension is precipitated by adding acetone to the mixture. The nanoparticles are washed by centrifuging with hexane and redispersing in ethanol for at least 2-3 cycles, and finally stored in ethanol.

#### Synthesis of 12.3 nm Pt nanoparticles

For 12.3 nm Pt nanoparticles, 40 mg  $\text{Pt}(\text{C}_5\text{H}_7\text{O}_2)_2$  and 30 mg polyvinylpyrrolidone (PVP,  $M_w = 40,000$ ) are dissolved in 5 ml ethylene-glycol, and sonicated for 30 minutes to get a homogenous solution. The solution was transferred into a three-necked round bottom flask, which was evacuated and purged with atmospheric pressure argon gas to get rid of additional oxygen and water. After three purging cycles, the flask was immersed into an oil bath heated to 200 °C under vigorous stirring of the reaction mixture as well as the oil bath. After 120 minutes of reaction, the flask was cooled down to room temperature. The suspension was precipitated by adding acetone to the mixture. The nanoparticles were collected by centrifuging. After precipitation, the particles were washed by centrifuging with hexane and redispersing in ethanol for at least 2-3 cycles, and finally stored in ethanol.

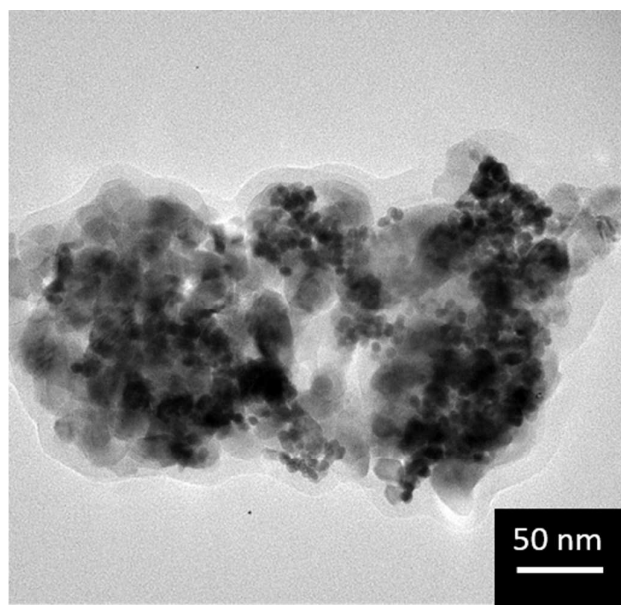


**Figure S6.** TEM image of a Pt/NiO composite (7.2 nm Pt) obtained at higher Pt loading.

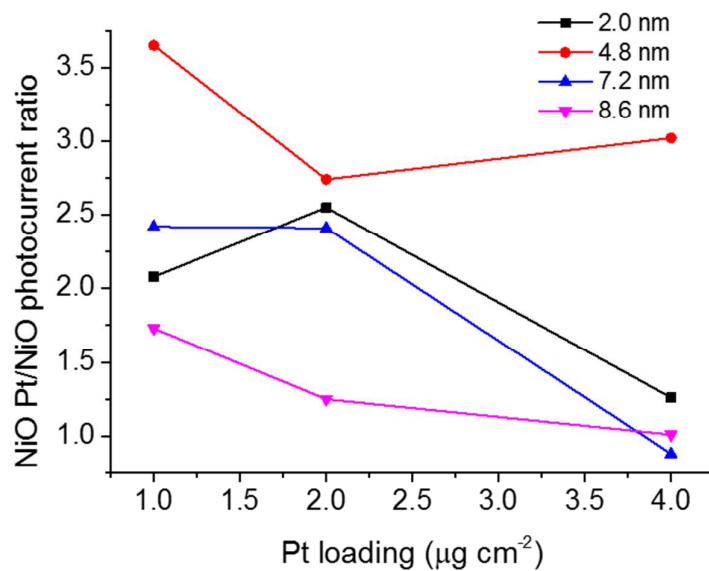


**Figure S7.** The effect of Pt size and concentration to the NiO Pt/NiO photocurrent ratio. Lines connecting the measured data are guides for the eye.

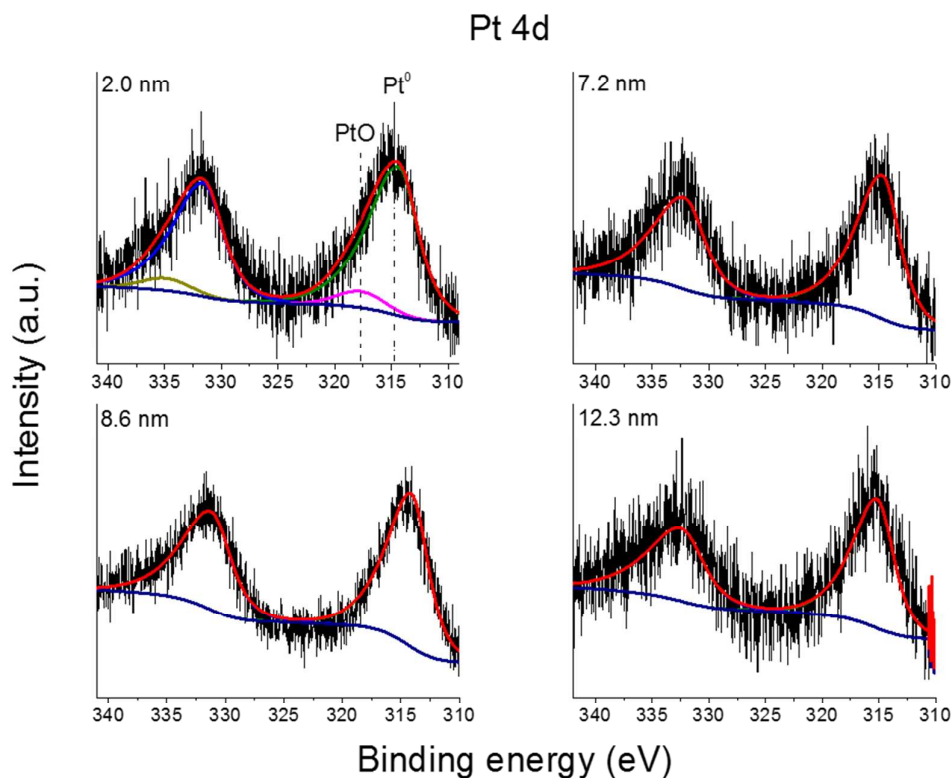


**Figure S8.** Pt 4d XP spectra of NiO/Pt nanocomposites with different Pt sizes ( $2 \mu\text{g cm}^{-2}$  loading).

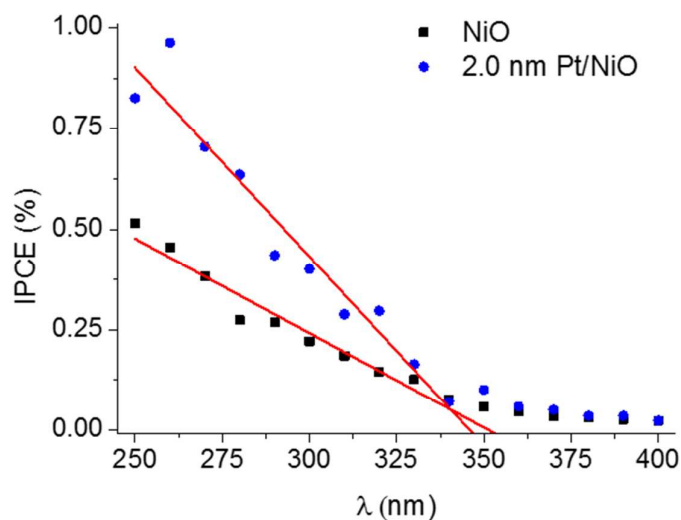


**Figure S9.** Photoaction spectra for the pristine NiO and 2.0 nm sized Pt decorated samples in 0.2 M  $\text{Na}_2\text{SO}_4$  electrolyte at  $E = -0.8 \text{ V}$ ,  $\Delta\lambda = 10 \text{ nm}$ .

#### EIS measurements:

Various equivalent circuits are proposed in the literature to fit metal-oxide nanostructures prepared via anodization. The common feature of these is the separation of the



response of the compact bottom and upper porous layer.<sup>5</sup> The response of the samples can be adequately fitted by an equivalent circuit. In this model both the bottom blocking layer and the upper porous layer in contact with the electrolyte are considered. The surface inhomogeneity of the electrodes was taken into account by substituting the capacitive elements in the model to constant phase elements. The equivalent circuit in Figure S10 was applied to evaluate the data from electrochemical impedance measurements. This circuit consists of an active solution (electrolyte) resistance ( $R_s$ ) coupled series with the impedance of the bottom compact NiO layer (CL) and the upper porous NiO layer (PL). Impedance of such electrodes is commonly described with parallel combination of the layer resistance ( $R_{CL}$  and  $R_{PL}$ ) and capacitance ( $Q_{CL}$  and  $Q_{PL}$ ).

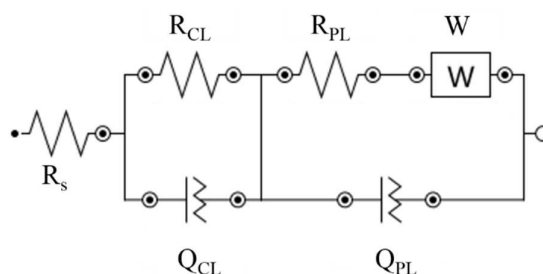


**Figure S10.** The equivalent circuit used for the EIS fits.

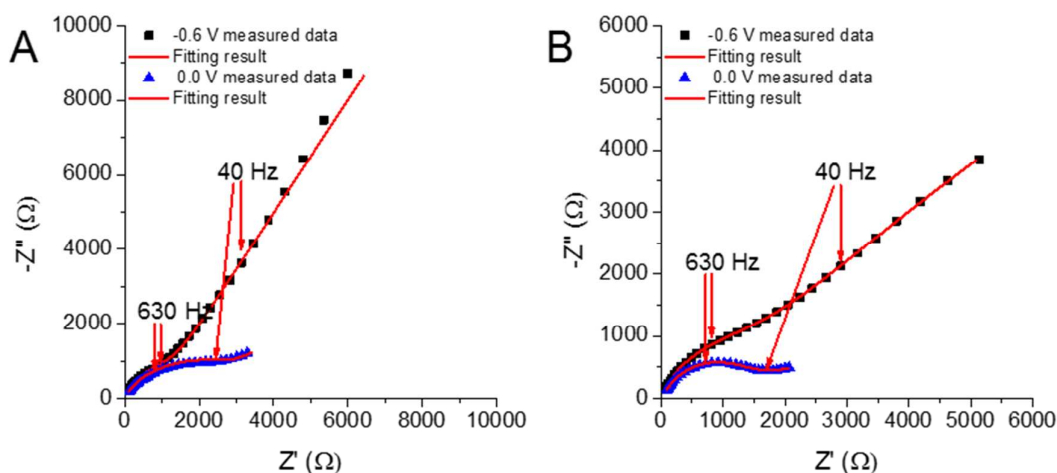


**Figure S11. A:** Electrochemical impedance spectra recorded for the bare NiO samples and fitted with the equivalent circuit in Figure S10 at two different potential  $E = -0.6$  V and  $E = -0.0$  V in the 10 Hz to 0.1 MHz frequency range in 1.0 M  $\text{Na}_2\text{SO}_4$ . **B:** Electrochemical impedance spectra recorded for the sample decorated with 8.6 nm Pt nanoparticles and fitted with the equivalent circuit in Figure S10 at two different potential  $E = -0.6$  V and  $E = -0.0$  V in the 10 Hz to 0.1 MHz frequency range in 1.0 M  $\text{Na}_2\text{SO}_4$ .

## References

- (1) Samu, G. F.; Pencz, K.; Janáky, C.; Rajeshwar, K. On the Electrochemical Synthesis and Charge Storage Properties of WO<sub>3</sub>/polyaniline Hybrid Nanostructures. *J. Solid State Electrochem.* **2015**, *19*, 2741–2751.
- (2) Macak, J. M.; Hildebrand, H.; Marten-Jahns, U.; Schmuki, P. Mechanistic Aspects and Growth of Large Diameter Self-Organized TiO<sub>2</sub> Nanotubes. *J. Electroanal. Chem.* **2008**, *621*, 254–266.
- (3) Shrestha, N. K.; Yang, M.; Schmuki, P. Self-Ordered Nanoporous Nickel Oxide/Fluoride Composite Film with Strong Electrochromic Contrast. *Electrochem. Solid-State Lett.* **2010**, *13*, C21-C24.
- (4) Jin, M.; Zhang, G.; Yu, F.; Li, W.; Lu, W.; Huang, H. Sponge-like Ni(OH)<sub>2</sub>–NiF<sub>2</sub> Composite Film with Excellent Electrochemical Performance. *Phys. Chem. Chem. Phys.* **2013**, *15*, 1601–1605.
- (5) Ali Yahia, S. A.; Hamadou, L.; Kadri, A.; Benbrahim, N.; Sutter, E. M. M. Effect of Anodizing Potential on the Formation and EIS Characteristics of TiO<sub>2</sub> Nanotube Arrays. *J. Electrochem. Soc.* **2012**, *159*, K83-K92.